Published in final edited form as:
Langmuir. 2012 September 11; 28(36): 12989–12998. doi:10.1021/la300724z.

Investigating ligand-receptor interactions at bilayer surface using electronic absorption spectroscopy and Fluorescence Resonance Energy Transfer

Navneet Dogra[a], **Xuelian Li**[a], and **Punit Kohli**[*]
Department of Chemistry and Biochemistry Southern Illinois University Carbondale, IL 62901

Abstract

We investigate interactions between receptors and ligands at bilayer surface of polydiacetylene (PDA) liposomal nanoparticles using changes in electronic absorption spectroscopy and Fluorescence Resonance Energy Transfer (FRET). We study the effect of mode of linkage (covalent versus non-covalent) between the receptor and liposome bilayer. We also examine the effect of size dependent interactions between liposome and analyte through electronic absorption and FRET responses. Glucose (receptor) molecules were either covalently or non-covalently attached at the bilayer of nanoparticles, and they provided selectivity for molecular interactions between glucose and glycoprotein ligands of *E. coli*. The receptor-ligand interactions between glucose and ligand on *E. Coli* surface induced stress on conjugated PDA chain which resulted in changes (blue to red) in the absorption spectrum of PDA. The changes in electronic absorbance also led to changes in FRET efficiency between conjugated PDA chains (acceptor) and fluorophores (Sulphorhodamine-101) (donor) attached to the bilayer surface. Interestingly, we did not find significant differences in UV-Vis and FRET responses for covalently- and non-covalently-bound glucose to liposomes following their interactions with *E. Coli*. We attributed these results to close proximity of glucose receptor molecules to the liposome bilayer surface such that induced stress were similar in both the cases. We also found that PDA emission from direct excitation mechanism was ~ 2 - 10 times larger than that of FRET based response. These differences in emission signals were attributed to three major reasons: non-specific interactions between *E. Coli* and liposomes; size differences between analyte and liposomes; and a much higher PDA concentration with respect to sulpho-rhodamine (SR-101). We have proposed a model to explain our experimental observations. Our fundamental studies reported here will help in enhancing our knowledge regarding interactions involved between soft particles at molecular levels.

Introduction

Molecular recognition events involving carbohydrates are very important in various biological processes such as functioning of the immune system[1] and in the interaction of viruses[2] and bacteria with cell. These recognition events usually involve communication between cells that is driven by specific interactions between molecules on the cell surfaces.[3] To study these receptor-ligand interactions for the molecular recognition, a wide variety of studies are reported in the literature.[4,5,6,7] The natural cell membrane, which has many

[*]pkohli@chem.siu.edu.
[a]equal contribution

Supplementary Materials. The supplementary materials provides information on fluorescence microscopic analysis, synthesis of monomers ***3*** and ***4***, procedure for the synthesis of nanoscale liposomes, Figures 1S to 6S. Estimation of number of liposomes/*E. Coli* is also provided in the supplementary materials. This information is available free of charge via the internet at http://pubs.acs.org.

highly specific molecular recognition receptor sites on its surface, may be considered a completely self-contained biosensing system where molecular recognition is directly linked to signal transduction.[6] When specific ligand binding occurs at these sites, the binding event is often transduced into a cellular message which can be communicated into cell or among many cells.[7] To mimic the complex molecular choreography of cell membrane in a simple way, many synthetic membranes are designed and prepared.[8,9] Conjugated polymer-based biosensor systems are a promising choice for cell membrane mimic because in these systems the signal of a specific ligand binding to the receptor in the bilayer can be transduced along the conjugated polymer chain.[6,7,8,9] The ligand-receptor interactions occurring at bilayer surface can affect the properties of the collective system producing larger signal amplification. [5,7,10,11,12,13]

Recently, polydiacetylene (PDA), a conjugated polymer, has been widely utilized as transducer because of its distinctive chromatic transition property and convenient preparation method through self-assembly and subsequent photopolymerization among diacetylene bonds.[14,15,16,17,18] It is well known that PDA shows intense blue color due to light absorption by its extended ene-yne conjugated backbone in the visible region. The torsion angle between substituent groups plays an important role in the appearance of conjugated polydiacetylene, as nearly flat structures are proposed to appear blue whereas strongly twisted structures appear red.[19] This structural/colorimetric transformation of PDA can be generated by various external stimuli, such as temperature[20,21], mechanical stress[22,23], pH[24], ionic strength[25], or bio-interactions[26,27]. It is demonstrated that by incorporating biological receptors in the PDA liposome bilayer, the binding of analytes to receptors may change the conformation of the polymer backbone providing a colorimetric response for a variety of biological targets[28,29]. To date, PDA has been successfully employed for the development of colorimetric biosensors for cholera toxin[30], influenza virus and bacteria[3132], epitopes[33], lipopolysaccharides[34], and phospholipase A_2[35]. Recently, oligopeptides-functionalized polydiacetylene liposomes were used as specific fluorescent sensor for bacterial lipopolysaccharides and *E. Coli* in aqueous solution.[36]

The emissive properties of PDA have potential for providing increased detection sensitivity and a lower detection limit compared to colorimetric sensors due to an inherent higher sensitivity of fluorescence. The development of fluorescence "*turn on*" sensors is a highly desirable and may also provide more sensitive approach for the detection of a target molecule.[37,38,39,40] In "*off*" state of these materials, the excited states propagating along the conjugated backbone are quenched when encountering an energy trap at an occupied receptor site which can lead to quenching of fluorescence. [4,7,41] Previously, we have demonstrated that the protein sensors based on fluorescence resonance energy transfer (FRET) between conjugated polymers and fluorophores can provide "*turn on*" sensors with high sensitivity and lower detection limit than those based on colorimetric change[42]. We demonstrated a novel FRET based system that utilizes changes in J value (spectral overlap) and changes in the quantum yield of the acceptors for fluorescence amplification[43,44].

The receptors containing lipids can be cross-linked through the use of diacetylene groups which form conjugated polymer backbone. It is also shown that naturally driven lipophilic molecules can be incorporated into PDA's bilayer membranes.[45] Several studies published in recent years have demonstrated that PDA liposomes and films with natural lipid assemblies intercalated within the polymer matrix also undergoes blue-red transitions in response to interactions with varied analytes.[46,47,48] Glucose molecules present at the surface of liposomes were previously used as receptors for the glyco-protein on *E. Coli* surface.[36,32,49] *E. coli*, a Gram-negative bacterium, usually uses fimbrial adhesions to bind or adsorb to the surface of host cells. For *E. coli* P fimbriae, recognizing the galactose-containing receptors[50]; type 1 fimbriae, binding to mannose-containing receptors[51]; S

fimbriae, recognizing sialyl(α2-3)galactosides[52]; G fimbriae, binding preferentially to terminal N-acetyl-D-glucosamine residues[53]. In particular, the cell surface glycolipid-conjugates seem to be important mediators of adhesion of *E. coli*.[54] In general, *E. Coli* interacts with glucose but these interactions are not as selective as compared to those present in the case of antibody and antigen. In the present case, use of glucose on the liposome surface presents a convenient way of probing the interactions between liposomes and *E. Coli*.

In a recent work, we found that the interactions between covalently bonded receptors on liposome surface and protein ligands appeared to induce a larger stress on the PDA backbone (hence, possessed a higher response) than those involved in non-covalently bonded receptors[42]. The main focus of the present work is to investigate the effect of covalently versus non-covalently attached receptors to the PDA liposome on the UV-Vis and FRET responses. We synthesized two different glucose-tagged lipids (***3*** and ***4*** in Scheme 1) to investigate the effect of covalently- and non-covalently PDA bounded receptors for investigating FRET response after binding of glucose with *E. Coli*. In the case of ***3***, the glucose was tagged to a long alkyl chain fatty acid, and the glucose residue was non-covalently inserted into bilayer of the liposomes (denoted by ***N***). For liposomes prepared with ***4***, the glucose residue was covalently linked to a diacetylene monomer that formed the conjugated backbone of liposomes after photopolymerization (denoted by ***C***). In all the experiments, sulfo-rhodamine-101 (SR-101, ***2***) and PDA (blue) were served as energy-donor and -acceptor respectively (Figures 1C). The changes in spectral overlap (***J***) value between the SR-101 emission and PDA absorption were observed after the addition of *E. Coli* to a glucose-containing liposome solution (Figures 1C, 1D and 3S). These changes in *J* values resulted in changes in SR-101 emission (Figure 1B and 1S(B)) signal which provided a convenient way of observing interactions between *E. Coli* and liposomes in solution.

In this manuscript, we investigate ligand-receptor interactions at bilayer using fluorescence resonance energy transfer between sulfo-rhodamine 101 (SR-101) donor (***2***) molecules and polydiacetylene acceptor molecules (Figure 1C and 1S(C)) after binding of glucose receptors attached to the surface of liposomes with protein ligands on *E. Coli*. To visualize the liposome-*E. coli* interactions, we prepared glucose receptors containing Giant Unilamellar Vesicles (GUVs) for fluorescence microscopic analysis (please see supporting material (SM)) for more information). We have employed optical spectroscopic (UV-Vis, emission, and FRET) and fluorescence microscopic techniques for investigating ligand-receptor interactions at the bilayer-aqueous interface.

Experimental section

Chemicals and Materials

N-Boc-L-threonine (>98%), acetobromo-α-D-glucose (>95%), iodine (>99.8%), potassium carbonate (anhydrous, >99%), trifluoroacetic acid (> 98%), were purchased from Aldrich. Triethylamine (>98%) and acetonitrile (MeCN) were purchased from Acros; dichloromethane (DCM), diethyl ether, chloroform (TCM), methanol (MeOH) and ethyl acetate (EtOAc) were purchased from Fisher Scientific. Solvents were purified and dried by distillation after refluxed with calcium hydride (CaH_2) and stored under Ar. Sulforhodamine-PDA (***2***) was synthesized according to a previously reported method. [40,44]. Scheme 1 shows the chemical structures of lipids and monomers used in our experiments.

Giant Unilamellar Liposome (GUVs)[55]

Besides the use of nanoscale liposomes, we have used GUVs (~15-60μm) for the studies involving the liposome-*E. coli* interactions using fluorescence microscopy. The use of GUVs provided an excellent way to visually probe the interactions of liposomes with *E. Coli*. These studies clearly show that the liposomes are attached to *E. coli* and also provided useful information on *E. Coli* distribution on the surface of GUVs. The self-assembled GUVs were prepared by using a mixture of 10,12-pentacosadiynoic acid (***1***), glucose-tagged lipid (***4***) and rhodamine-tagged DMPC (***6***) [1,2-dioleoyl-*sn*-glycero-3-phosphoethanolamine-N-(lissamine-rhodamine-B-sulfonyl) (ammonium salt)].

GUVs were synthesized according to following procedure[55, 56]

Briefly, a mixture containing ***1***, ***4*** and ***6*** in a desired ratio (4 : 4 : 2) was dissolved in chloroform in a round bottom flask. The total concentration of all the monomers was 1 mM in the final solution. The solution was passed through a 0.45 μm nylon filter to remove the lipid aggregates. The solvent was then evaporated completely. The dried mixture was again dissolved in a mixture of 3 mL of chloroform and 1 mL of methanol. The aqueous phase (25 mL of nanopure water) was then added carefully along the flask walls. The organic solvent was removed in a rotary evaporator under reduced pressure, and an opalescent fluid was obtained. The resultant solution is cooled at 4 °C overnight to promote self assembly of monomers.

E. Coli staining with 4′,6-diamidino-2-phenylindole (DAPI) fluorophore

E. coli was stained with DAPI fluorophore for fluorescence microscopic studies. DAPI is a well-known agent that selectively stains nuclei.[57] The staining of *E. Coli* was performed according to a reported procedure[58]. Briefly, 5 mL aliquots of *E. coli* were taken from stock bacterial culture. The aliquot was transferred to centrifuge tube to which equal amount of PBS was added. The solution was centrifuged for 15 min at 8000 rpm, the supernatant was discarded and equal volume (1 μM) of DAPI was added to the remaining solution. The solution mixture was then centrifuged for 15 min and supernatant was removed. Equal amount of PBS was added again to the bacterial solution prior to and before centrifugation. This process was repeated 3 times. DAPI-tagged *E. Coli* were stored in refrigerator for future uses. The interaction between *E. Coli* and liposomes were investigated using fluorescence microscopy (please see SM).

Spectroscopic Measurements

PDA liposomes ***C*** (covalently-bound glucose) and ***N*** (non-covalently bound glucose) contained 5 to 20% glucose-lipid (***3***) or glucose-PDA (***4***) respectively were incubated with different concentrations (between 0.033×10^7 to 3.3×10^7 cells/mL) of *E. coli* in deionized water for 30 min at room temperature. UV-Vis absorption spectra of all of the samples were recorded using a Perkin Elmer Lambda 25 (spectral slit width 1 nm) UV-Vis spectrophotometer. The color transition of the PDA liposome solution was observed by comparing two main absorption maxima of blue- and red-PDA forms at 540 and 640 nm respectively. The colorimetric response (CR) is calculated as a percent change in blue to red color after incubated the samples with different concentration of *E. coli* solution as shown in Eqs. 1 and 2[31].

$$CR = \frac{(PB_0 - PB)}{PB} * 100\%$$

$$PB = \frac{A_{640}}{A_{540} + A_{640}} * 100\%$$

PB and PB_0 are blue and red-PDA ratios of a sample after and before addition of *E. coli*, respectively. A_{640} and A_{540} represent the absorbance values at wavelengths of 640 nm and 540 nm, respectively.

The emission spectra were measured using a Photon Technology International spectrofluorometer. For all emission spectra, the excitation wavelengths for SR-101 and PDA were set at 560 nm and 490 nm respectively, and the spectral slit widths (both excitation and emission) were 6 nm. Under these conditions, the contribution of emission from PDA to total emission and that of SR-101 to total emission was minimum when excited at 560 nm and 490 nm respectively.

Result and discussion

Absorption spectroscopy of PDA liposomes with addition of E. Coli

Polymerized liposomes appeared blue in color and exhibited an intense absorption maximum at ~640 nm along with less intense peaks centered at590 nm (Figures 1A and 1S(A)). The peaks centered at 640 nm and 590 nm are attributed to *0-0'* and *0-n'* vibration transitions in π-π^* electronic transition respectively of the blue-form of PDA.[59] The blue-shifted peak centered at ~540 nm is attributed to red-form of PDA. We did not observe this peak in our previous reports [42,43,44] where the ligands were small and were present away from aqueous-bilayer interface. The low-intensity peak at 540 nm (Figures 1A and 1S(A)) resulted from stress induced on conjugated PDA due to cross-sectional area mismatch between glucose and carboxylic acids that led to changes in the bilayer packing density.[14] It is interesting to see that at higher concentration of *E. Coli*, the increase in the absorbance in the 400-450 nm region was much larger than the rest of the spectrum (Figures 1A and 1S(A)). This large increase in the absorbance is due to scattering of the light due to binding of *E. Coli* with liposomes which significantly increases the size of the particles present in the solution[60]. One of the consequences of this increase in the absorbance led to significant errors in the calculations of spectral overlap (*J*). Based on our recent work[61], we would like to emphasize that the calculations of *J*, *E* and *CR* provide very useful qualitative information and our interpretations of the data do not change significantly due to errors resulted from light scattering.

With addition of *E. Coli* to PDA solution, the blue absorption peak was decreased and the intensities of the red absorption peaks (centered at 490 nm and 540 nm) were increased (Figures 1A and 1S(A)). The color of the liposome solution turned purple and then red with increasing concentration of *E. coli* in the solution. These blue to red chromatic transition presumably is attributed to applied stress on the PDA backbone following interactions between glucose and surface proteins on *E. Coli*. These interactions led to reduced effective conjugated length of the PDA backbone chains which shifted the electronic absorption band to shorter wavelengths.[26,32,33] To evaluate the effect of receptor concentration on the sensor response, we calculated *CR* (%) values and emission signal for a range of glucose receptors containing liposomes. Figures 2A and 2S(A) show *CR*-versus-*E. Coli* concentration curves for liposomes with three different receptor concentrations of ***3*** and ***4*** respectively on the liposome surface. The *CR* values of both series (***C*** and ***N***) increased with an increase in the *E. coli* concentration in the solution. At 3.3×10^7 *E. coli* particles/mL in aqueous solution, the *CR* values were ~32 and ~34 for liposomes ***C*** (15% of ***3***) and ***N*** (15% of ***4***) respectively. These *CR* values are much higher than *CR* ~ 8.1 for control experiments under same *E. Coli*

concentration for the liposomes that did not contain glucose receptors on their surface. The subtle non-specific interactions (such as hydrophobic and electrostatic interactions) between *E. Coli* and liposomes appears to contribute to CR ~ 8.1 in the control experiments. Further, we did not observe a significant color change to a liposome solution when a BSA protein solution containing 150 μg/mL was added to ***C*** and ***N*** liposome solutions. These experiments agree with our argument that the bio-recognition interactions between glucose and *E. Coli* dominantly contributed to larger *CR* values whereas the samples without specific interactions between *E. Coli* and receptors showed much smaller CR values. In both the cases, the incorporation of glucose receptors covalently or non-covalently in the liposomes enhanced the colorimetric response due to specific interaction of glucose at the liposome surface with surface ligands on *E. coli* cell wall. As the concentration of glucose (***3*** or ***4*** concentration) in the liposomes increased, the *CR* values of the solution also increased upon the addition of *E. coli*. The CR values for the liposome ***C*** and ***N*** series were almost same.

Emission spectra of glucose-tagged liposomes with addition of E. Coli

In our previous studies of biotin-streptavidin interactions using a similar PDA system, we observed that the covalently bound receptors on the surface of liposomes (***C***) showed much larger (~2-3 times) response after interactions with protein ligands than for liposomes composed with surface receptors that were non-covalently (***N***) linked to the bilayer[42]. We hypothesized that the induced stress due to biotin-streptavidin interactions on PDA backbone chains was higher for liposomes composed with receptor molecules covalently attached to the backbone of the PDA than for liposomes composed with non-covalently inserted receptors in the bilayer of the liposomes. Thus, the enhanced stress transport was hypothesized to result in larger changes in both colorimetric and FRET signals for liposomes with covalently-bound receptors to the surface of the liposomes. For biotin-streptavidin PDA liposome system, the size of streptavidin (analyte) was much smaller than that of liposomes, and a large portion or whole surface of the liposomes is accessible to streptavidin (Figure 4S). However in the present studies, *E. Coli* (analyte) is much larger than nanoscale liposomes.

The emission spectra of liposomes ***N*** and ***C*** upon addition of various concentration of *E. coli* are shown in Figures 1B and 1S(B) respectively. The emission intensity of SR-101 increased gradually with the increasing concentration of *E. coli*. This is consistent with our UV-Vis spectroscopic analysis and the design of our system that the quenching of emission of SR-101 will be reduced due to decrease in the spectral overlap (*J*) between SR-101 and PDA after addition of *E. Coli* to the liposome solution. A decrease in the FRET efficiency and increase in the SR-101 emission was observed following *E. Coli* addition to the solution (Figures 2B and 2S(B)). We estimated FRET efficiency (*E*), *J* and changes in *J* (Δ*J*) using the following equations:[62]

$$E = \frac{(F_0 - F)}{F_0}$$

where *F* and F_0 is the emission intensity of donor in the presence and absence of the acceptor (PDA). F_0 here means emission intensity of SR 101 when PDA was unpolymerized.

$$\mathrm{J} = \int_0^\infty \mathrm{J}(\lambda)\,\mathrm{d}\lambda = \int_0^\infty \mathrm{PL}_{D-\mathrm{corr}}(\lambda)\,\varepsilon_A(\lambda)\,\lambda^4 d\lambda$$

where $PL_{D\text{-}corr}$ and ε_A represent the donor emission (normalized dimensionless spectrum) and molar absorption coefficient of the acceptor.

$$\Delta J = \frac{(J - J_0)}{J_0} \times 100\%$$

where J_0 and J are the donor-acceptor spectral overlap of sample before and after addition of *E. coli*, respectively.

Trend of electronic absorption and FRET responses with E. Coli concentration

The present study investigates the effect of molecular recognition between molecules at bilayer interfaces of liposomes and *E. Coli* on changes in electronic absorption of PDA and FRET responses. We have used colorimetric response (*CR*), ΔJ, and FRET responses to evaluate interactions between liposomes and *E. Coli*. *CR* is a measure of changes in the electronic absorbance of blue-PDA after *E. Coli*, ΔJ provides a measure of integrated area between the spectral overlap between PDA absorbance and SR-101 emission curves, and it depends on PDA absorbance changes. The changes in the PDA conformations provide an overall transfer probability that is changed as a consequence of conformational changes of PDA. Finally, ΔE represents changes in the FRET efficiency as a result of spectroscopic changes in the PDA absorbance spectrum. We observed that all three responses (*CR*, ΔE *and* ΔJ,) show similar trend with increase of *E. Coli* in the solution (Figures 2, 2S and 3S). For example, there is a rapid increase in response followed by plateau for all three response-[*E. Coli*] curves. These trends were reproducible for different liposome preparations. The magnitude of these responses was also similar for liposomes composed with ***3*** and ***4***. For example, whereas ΔJ was 18% and 24% for liposomes with 15% ***3*** and ***4*** respectively (Figure 3S), *E* was ~20% for these liposomes (Figure 2B and 2S(B)). The estimated values of ΔJ contains some error due to scattering contribution in the absorption spectra (please see above). However, for all purposes, ΔJ for both the systems (***C*** and ***N***) were similar in values. The shape of the response trend is not unexpected because the underline molecular phenomenon that contributes to these three responses is stress induced on the PDA backbone due to interactions of *E. Coli* with liposomes. The molecular interactions between glucose and *E. Coli* presumably resulted in stress that is transported to conjugated polydiacetylene chain. The application of this subtle molecular stress on the PDA backbone led to blue-shift in the UV-Vis spectrum of PDA and a decrease in the spectral overlap (*J*) between the emission of SR-101 and absorption of PDA. Overall, the result of *E. Coli*-liposome binding led to decrease in the quenching SR-101 fluorophores, that is, the emission from SR-101 emission was enhanced (Figures 1B and 1S(B)).

During the initial additions of *E. Coli*, the liposome bilayer was enriched with glucose receptors that were steric unhindered for binding with *E. Coli*. The ratio of number of glucose receptors to binding protein on *E. Coli* was large in the beginning of the experiments, and *E. Coli* can access to glucose receptors on the liposome surface. Due to these reasons, the responses due to binding of liposomes with *E. Coli* were sharp in the initial stages of addition of *E. Coli* to the liposome solution (Figure 2A and 2S). However, with increase in the *E. Coli* concentration in the solution, many protein ligands on *E. Coli* surface were occupied, and both the number of available glucose receptors on the liposome surface and glycol-protein on *E. Coli* were significantly reduced as well. This led to decrease in the probability of glucose-*E. Coli* interactions which resulted in a slower rise of responses at later stages of the experiment.

Interestingly, irrespective of receptor concentration in the liposomes, the responses appear to be saturated at around 1×10^7 *E. Coli*/mL (Figure 2 and 2S). The saturation of the response

means that further increase in the number of interactions between liposome and *E. Coli* appears small. The dimension (both length and diameter) of *E. Coli* can depend upon the strain of *E. Coli*, *E. Coli* was ~2 μm long with a diameter of ~500 nm in our experiment.[58] Assuming the mono-dispersed distribution of liposomes with an average diameter of about 250 nm,[68] the number of liposomes were ~ 4.19×10^{10}/mL of the solution (please see SM for more information). This means on average total number of molecules and glucose in a liposome are ~ 2.9×10^6 and 1.45×10^5 respectively. We estimated that each *E. Coli* on an average interacted with ~40 liposomes that contain 10 mol% glucose concentration on their surfaces. This corresponds to only ~ 1% of the total surface area is covered with liposomes under our experiment conditions. Interestingly, the signal (both E and R_{FRET}) in our experiments get saturated at a concentration of ~ 10^7 *E. Coli* in the solution. Increase in CR values for similar experiments was larger, however, as we noted earlier, due to scattering in the UV-Vis spectra the interpretation of these results are qualitative in nature. These estimates suggested that assuming the whole surface of *E. Coli* was accessible to liposomes for interactions under our experimental conditions, the signal generated following *E. Coli*-liposome interactions is less sensitive to *E. Coli* concentration > 1×10^7 particles/mL. One of the reasons for saturation in signal response is attributed to insufficient number of receptors on the liposome surface for interactions with *E. Coli*. This is also evident from our experimental data: when the concentration of glucose in the liposomes was increased from 5 mol% to 15 mol%, the increase in both E and R_{FRET} responses was modest with increase in *E. Coli* concentration from 1×10^7 particles/mL to 3.3×10^7 particles/mL as compared to a much larger signal enhancement when *E. Coli* concentration was increased from 0 particle/mL to 1×10^7 particles/mL. The available ligand density on *E. Coli* surface is also not known, therefore, it is not possible to estimate with certainty how much further enhancement in the signal can be achieved with increase in the glucose concentration in the liposomes.

In these calculations, we have assumed that (1) *E. Coli* are cylindrical in shape with hemi-spheres at its two ends; (2) the concentration of glucose on the liposomes are evenly distributed and that half of them are inside of the liposomes which were not available for binding to *E. Coli*; (3) liposomes are mono-dispersed; and (4) only half of the glucose molecules on the outer surface of the liposomes interacted with *E. Coli* through specific glucose *E. Coli* interactions. The last assumption is valid because we have not observed *E. Coli* aggregation in the solution under our experimental conditions. There is also a possibility that liposomes are able to interact with multiple *E. Coli* but due to significantly large size of *E. Coli* and a low concentration of liposomes in the solution, we believe that there is a large steric hindrance for two or more *E. Coli* to bind with a same liposome attached on to a given *E. Coli*. Figures 3A and 3B show the fluorescence micrograph of liposomes tagged with SR-101 and *E. Coli* stained with DAPI respectively. For these experiments, the number of *E. Coli* were in excess (>20 times) as compared to number of GUVs. Our fluorescence microscopic data showed that whole surface of GUVs liposomes is accessible to *E. Coli* although some spots on liposomes appeared to have an aggregation of *E. Coli* which is believed to be result of an excess of *E. Coli* relative to liposomes in the solution (Figures 3A, 3B, and 3C). Further, we have also performed binding of *E. Coli* with nanoscale liposomes using fluorescence microscopic analysis (Figure 3D). Interestingly, in the later case, the size of liposomes was much smaller than that of *E. Coli*, and the liposomes (which were in excess) bound to *E. Coli* surface. The red emission around the blue fluorescent *E. Coli* indicated bound liposomes. Analysis with both smaller and larger liposomes confirmed the binding of liposomes with *E. Coli* (Figure 3).

We believe that the fourth assumption needs more discussion. For our experiments, the glucose receptors are present very near to the surface of the liposomes (please see chemical structures in Scheme 1). Although our experiments suggested that the presence of glucose on the liposome surface is necessary for response, however, once *E. Coli* is attached with

liposomes, non-specific surface interactions between *E. Coli* and liposomes cannot be ruled out. This is because the binding of liposomes and *E. Coli* is very close to the surface of liposomes and that both the *E. Coli* and liposomes are soft particles which can be easily deformed (Figures 4 and 4S). Further, these non-specific interactions between *E. Coli* and liposomes deform conjugated polymer chain in the PDA liposomes. One of the consequences of binding of liposomes with *E. Coli* through these non-specific interactions is large PDA emission signal through direct excitation mechanism (Figure 5) (please see more discussion below).

Finally, with increase in the glucose receptor concentration in the liposomes, the initial response (slope between the response and *E. Coli* concentration at the beginning of the experiment) was larger than that for particles with a lower receptor concentration (Figures 2A and 2S (A)). This is because larger number of glucose receptors interacted with *E. Coli* producing enhanced stress on the conjugated PDA chain.

Direct-versus-FRET response

We now compare the emission of the direct excitation of PDA-versus-FRET response. It is interesting and important to compare the emission from SR-101 and red-PDA to the total emission intensity when excited at different wavelengths. This discussion also shed some light on specific-versus-non-specific interactions between liposomes and *E. Coli*. For direct excitation, we meant excitation of PDA chains at 490 nm, and the emission was observed in 510 nm – 700 nm region (Figure 6S). For FRET experiments, the excitation was performed at 560 nm, and the emission was collected in 570 -700 nm region (Figures 1B and 1S(B)). Previously, we have observed a smaller emission response for direct excitation as compared to FRET mechanism for a PDA system in which biotin was tagged on to liposome surface and the response was induced from biotin-streptavidin interactions.[42] In contrast to our previous results, however, in the present study we observed a much higher emission response (>10 times) for PDA direct excitation (Figures 5A,5B and 5S) than the emission response due to FRET mechanism (Figures 1B, 5S(A) and 5S(B)). Figures 5 and 5S show $R_{FRET,N}$ and $R_{FRET,C}$, which represents ratio of SR-101 emission in the presence and absence of *E. Coli*. In both of these cases, the maximum FRET ratio for *N* and *C* series was ~2. That is, the maximum increase in the FRET emission of SR-101 after addition of *E. Coli* to the liposome solution was ~ 2. However, under the same conditions, the maximum increase in R_{Direct} of PDA was > 10 for liposomes prepared with ***3*** and ***4*** after *E. Coli* was added to the liposome solution (Figures 5B and).

We would like to emphasize *E* value of ~ 34% (for 20 mol% of glucose receptors) was calculated using Eq. 3 where F_0 corresponds to emission intensity of SR 101 for the unpolymerized PDA liposomes (in the absence of acceptor), and *F* is the emission intensity of liposomes after addition of *E. Coli* in the solution. R_{FRET} represents a different measure of decrease in FRET in our experiments. It is calculated by dividing emission intensity of SR 101 in the presence and absence of *E. Coli*, but in all of R_{FRET} calculations the FRET mechanism was present. The major difference between *E* and R_{FRET} is that the F_0 value in *E* calculations does not possess FRET component whereas the emission intensity in all R_{FRET} calculations contains a FRET component.

In general, the emission intensity for direct excitation depends on concentration (C) of PDA, its excitation coefficient (ε) and quantum yield (Q_y). FRET emission response, on the other hand, depends upon the FRET efficiency (*E*) between SR-101 and PDA along with quantum yield (Q_y) of the emitting specie (SR-101). In our case, the Q_y and ε of SR-101 are ~ 3-4 and 2-3 orders of magnitude higher than red PDA, whereas *E* ranges between 10 and 34% (Figures 2B and 2S(B)). PDA concentration is about 10^6 times larger than that of SR-101 concentration. A much larger direct emission response compared to FRET response in our

studies is attributed to two major contributions: First, although both Q_y and ε of SR-101 are significantly larger than that of PDA, the overall PDA concentration in liposomes is three orders of magnitude larger than that of SR-101. This large concentration differences between PDA and SR-101 compensated for lower Q_y and ε of PDA. *E. Coli* is much larger than liposomes, thus, about half of the total glucose receptors can interact with surface proteins of the *E. Coli* under our experimental conditions. This means that FRET response in glucose-*E. Coli* system is obtained from ~ half of the available glucose receptors. Second, our calculations suggested that only ~1% of *E. Coli* surface is occupied by the liposomes, and rest of the surface is available for specific and/or non-specific interactions. These non-specific interactions presumably induced stress on PDA backbone leading to conformation changes in the conjugated PDA chain without affecting FRET response from other half of the liposome surface which is not in contact with *E. Coli* (Figure 4 and 4S). We believe that these non-specific interactions are a major contributor to the PDA emission signal from direct excitation but they do not contribute significantly to the FRET response. We also note that for this to happen, the first step is specific binding of glucose with *E. Coli*. Without this step, the possibility of proposed non-specific interactions is small. This is observed in our control experiments that the emission response is negligible in the absence of glucose receptors on the liposome surface (Figures 1B and 1S(B)), Thus, the size differences between analyte and liposomes, a much higher PDA concentration with respect to SR-101, and non-specific interactions between *E. Coli* and liposomes contributed to a much larger direct emission signal than as compared to the FRET response.

Conclusions

In summary, we have investigated interactions between *E. Coli* and glucose-tagged liposomal nanoparticles using changes in electronic absorption spectroscopy and FRET response. The glucose groups on the liposome surface provided selectivity through interactions between carbohydrate and *E. coli*. We did not find significant differences in UV-Vis and FRET responses between covalently- and non-covalently-bound glucose to liposomes following their interactions with *E. Coli*. We attributed these results to close proximity of glucose receptor molecules to liposome bilayer surface such that induced stress due to receptor-ligand interactions were similar in both the cases. We also found that PDA emission from direct excitation mechanism was ~5 times larger than FRET based response. We attributed these differences in emission signals to three major reasons: non-specific interactions between *E. Coli* and liposomes; size differences between analyte and liposomes; and a much higher PDA concentration with respect to SR-101. This system has implications in several biosensing applications where low cost and sensitivity are the top priorities.

Supplementary Material

Refer to Web version on PubMed Central for supplementary material.

Acknowledgments

We acknowledge financial support from the National Science Foundation (CAREER award) and the National Institute of Health (GM 8071101). Drs. John Bozzola and Steve Schmitt, and Ms. Hillary Gates (IMAGE center at SIUC) helped us in the electron microscopy analysis. We acknowledge Mr. Kunal Chatterjee and Prof. Ramesh Gupta for providing *E. Coli*. Ms. Julia Reyes helped us in liposome preparation. We would like to acknowledge positive critics of three anonymous reviewers which made the manuscript stronger after revisions.

References

1. Karlsson KA. Microbial recognition of target-cell glycoconjugates Curr. Opin. Struct. Biol. 1995; 5:622.

2. Guo CX, Boullanger P, Liu T, Jiang L. Size effect of polydiacetylene vesicles functionalized with glycolipids on their colorimetric detection ability. J. Phys. Chem. B. 2005; 109:18765–18771. [PubMed: 16853414]
3. Sharon N, Lis H. Lectins as cell recognition molecules. Science. 1989; 246:227. [PubMed: 2552581]
4. Spevak W, Nagy JO, Charych DH. Molecular assemblies of functionalized polydiacetylenes. Adv. Mater. 1995; 7:85–89.
5. Kim TH, Swager TM. A fluorescent self-amplifying wavelength-responsive sensory polymer for fluoride ions. Angew. Chem. Int. Ed. 2003; 42:4803.
6. Pan J, Charych D. Molecular Imaging of Thermochromic Carbohydrate-Modified Polydiacetylene Thin Films. Langmuir. 1997; 13:1365–1367.
7. Lehninger, Albert L.; Nelson, David Lee; Cox, Michael M. Lehninger principles of biochemistry. Volume 4:238–268.
8. Zhang SW, Swager TM. Fluorescent detection of chemical warfare agents: functional group specific ratiometric chemosensors. J. Am. Chem. Soc. 2003; 125:3420. [PubMed: 12643690]
9. Wiskur SL, Ait-Haddou H, Lavigne JJ, Anslyn EV. Teaching old indicators new tricks. Acc. Chem. Res. 2001; 34:963. [PubMed: 11747414]
10. Wang S, Gaylord BS, Bazan GC. Fluorescein provides a resonance gate for FRET from conjugated polymers to DNA intercalated dyes. J. Am. Chem. Soc. 2004; 126:5446–5451. [PubMed: 15113216]
11. Chen RF. Dansyl labeled proteins: determination of extinction coefficient and number of bound residues with radioactive dansyl chloride. Anal. Biochem. 1968; 25:412–416. [PubMed: 5704757]
12. Lee K, Rouillard J-M, Pham T, Gulari E, Kim. Signal-amplifying conjugated polymer-DNA hybrid chips. J. Angew. Chem. Int. Ed. 2007; 46:4667.
13. Wang S, Gaylord BS, Bazan GC. Collective Optical Behavior Of Cationic Water-Soluble Dendrimers. Adv. Mater. 2004; 16:2127.
14. Okada S, Peng S, Spevak W, Charych D. Color and Chromism of Polydiacetylene Vesicles. Acc. Chem. Res. 1998; 31:229–239.
15. Carpick RW, Sasaki DY, Burns AR. First Observation of Mechanochromism at the Nanometer Scale. Langmuir. 2000; 16:1270.
16. Morigaki K, Baumgart T, Jonas U, Offernhausser A, Knoll W. Photopolymerization of Diacetylene Lipid Bilayers and Its Application to the Construction of Micropatterned Biomimetic Membranes. Langmuir. 18:4082.
17. Huo Q, Russel KC, Leblanc RM. Chromatic Studies of a Polymerizable Diacetylene Hydrogen Bonding Self-Assembly: A “Self-Folding” Process To Explain the Chromatic Changes of Polydiacetylenes. Langmuir. 1999; 15:3972.
18. He H, Mortellaro MA, Leiner MJP, Fraatz RJ, Tusa JK. A fluorescent sensor with high selectivity and sensitivity for potassium in water. J. Am. Chem. Soc. 2003; 125:1468. [PubMed: 12568593]
19. bastien Filhol, Jean-Se; Deschamps, Je rome; Dutremez, Sylvain G.; Boury, Bruno; Barisien, Thierry; Legrand, Laurent; Schott, Michel. Polymorphs and colors of polydiacetylenes: a first principles study. J. Am. Chem. Soc. 2009; 131:6976–6988. [PubMed: 19413321]
20. Burns AR, Sasaki D, Shelnutt J, Brinker CJ. Self-assembly of mesoscopically ordered chromatic polydiacetylene/silica nanocomposites. Nature. 2001; 410:913. [PubMed: 11309612]
21. Wenzel M, Atkinson GH. Chromatic properties of polydiacetylene films. J. Am. Chem. Soc. 1989; 111:6123.
22. Rubner MF. Synthesis and characterization of polyurethane-diacetylene segmented copolymers. Macromolecules. 1986; 19:2129.
23. Tashiro K, Nishimura H, Kobayashi M. First Success in Direct Analysis of Microscopic Deformation Mechanism of Polydiacetylene Single Crystal by the X-ray Imaging-Plate System. Macromolecules. 1996; 29:8188.
24. Cheng Q, Stevens RC. Charge-Induced Chromatic Transition of Amino Acid-Derivatized Polydiacetylene Liposomes. Langmuir. 1998; 14:1974.

25. Kolusheva S, Shahal T, Jelinek R. Cation-Selective Color Sensors Composed of Ionophore–Phospholipid–Polydiacetylene Mixed Vesicles. J. Am. Chem. Soc. 2000; 122:776–780.
26. Nie Q, Zhang Y, Zhang J, Zhang M. Immobilization of polydiacetylene onto silica microbeads for colorimetric detection. J. Mater. Chem. 2006; 16:546.
27. Wang C, Ma Z, Su Z. Highly sensitive gas sensors based on hollow SnO_2 spheres prepared by carbon sphere template method Sens. Actuators, B. 2006; B113:510.
28. Kim JM, Ji EK, Woo SM, Lee H, Ahn DJ. Immobilized Polydiacetylene Vesicles on Solid Substrates for Use as Chemosensors (pages 1118–1121). Adv. Mater. 2003; 15:1118–1121.
29. Ma G, Cheng Q. A Vesicular Polydiacetylene Sensor for Colorimetric Signaling of Bacterial Pore-Forming Toxin. Langmuir. 2005; 21:6123–6126. [PubMed: 15982007]
30. Charych DH, Cheng J, Reichert A, Kuziemko G, Stroh M, Nagy JO, Spevak W, Stevens RC. A 'litmus test' for molecular recognition using artificial membranes. Chem. Biol. 1996; 3:113. [PubMed: 8807836]
31. Charych DH, Nagy JO, Spevak W, Bednarski MD. Direct colorimetric detection of a receptor-ligand interaction by a polymerized bilayer assembly. Science. 1993; 261:585–588. [PubMed: 8342021]
32. Ma ZF, Li JR, Liu MH, Cao J, Zou ZY, Tu J, Jiang L. Colorimetric Detection of *Escherichia coli* by Polydiacetylene Vesicles Functionalized with Glycolipid. J. Am. Chem. Soc. 1998; 120:12678.
33. Kolusheva S, Kafri R, Marina K, Jelinek R. Rapid colorimetric detection of antibody-epitope recognition at a biomimetic membrane interface. J. Am. Chem. Soc. 2001; 123:417–422. [PubMed: 11456543]
34. Rangin M, Basu A. Lipopolysaccharide identification with functionalized polydiacetylene liposome sensors. J. Am. Chem. Soc. 2004; 126:5038–5039. [PubMed: 15099065]
35. Okada S, Jelinek R, Charych DH. Color and Chromism of Polydiacetylene Vesicles. Angew. Chem. Int. Ed. 1998; 33:655–659.
36. Wu, Junchen; Zawistowski, Adam; Ehrmann, Michael; Yi, Tao; Schmuck, Carsten. Peptide functionalized polydiacetylene liposomes act as a fluorescent turn-on sensor for bacterial lipopolysaccharide. J. Am. Chem. Soc. 2011; 133:9720–9723. [PubMed: 21615123]
37. McQuade DT, Hegedus AH, Swager TM. Signal Amplification of a "Turn-on" Sensor: Harvesting the Light Captured by a Conjugated Polymer. J. Am. Chem. Soc. 2000; 122:12389.
38. Tong, Hui; Wang, Lixiang; Jing, Xiabin; Wang, Fosong. "Turn-On" Conjugated Polymer Fluorescent Chemosensor for Fluoride Ion. Marcromolecules. 2003; 36:2584.
39. Uchiyama S, Kawai N, Iwai K. Fluorescent polymeric AND logic gate with temperature and pH as inputs. J. Am. Chem. Soc. 2004; 126:3032. [PubMed: 15012116]
40. Liu B, Bazan C. Homogeneous Fluorescence-Based DNA Detection with Water-Soluble Conjugated Polymers. Chem. Mater. 2004; 16:4467.
41. Kuroda K, Swager TM. Self-amplifying sensory materials: Energy migration in polymer semiconductors. Macromol. Symp. 2003; 201:127.
42. Li, Xuelian; Kohli, Punit. J. Phys. Chem. C. 2010; 114:6255–6264.
43. Li X, McCarroll M, Kohli P. Modulating Fluorescence Resonance Energy Transfer in Conjugated Liposomes. Langmuir. 2006; 22:8615–8617. [PubMed: 17014092]
44. Li X, Malthews S, Kohli P. Fluorescence Resonance Energy Transfer in Polydiacetylene Liposomes. J. Phys. Chem. B. 2008; 112:13263–13272. [PubMed: 18816092]
45. Ma G, Cheng Q. Manipulating FRET with polymeric vesicles: development of a "mix- and-detect" type fluorescence sensor for bacterial toxin. Langmuir. 2006; 22:6743–6745. [PubMed: 16863214]
46. Orynbeyeva Z, Kolusheva S, Livneh E, Lichtenshtein A, Nathan I, Jelinek R. Visualization of membrane processes in living cells by surface-attached chromatic polymer patches. Angew. Chem. Int. Ed. 2005; 44:1092.
47. Evrard D, Touitou E, Kolusheva S, Fishov Y, Jelinek R. A new colorimetric assay for studying and rapid screening of membrane penetration enhancers. Pharm. Res. 2001; 18:943. [PubMed: 11496953]
48. Katz M, Ben-shlush I, Kolusheva S, Jelinek R. Rapid colorimetric screening of drug interaction and penetration through lipid barriers. Pharm. Res. 2006; 23:580. [PubMed: 16511676]

49. Ma, Zhanfang; Li, Jinru; Jiang, Long. Influence of the Spacer Length of Glycolipid Receptors in Polydiacetylene Vesicles on the Colorimetric Detection of Escherichia coli. Langmuir. 2000; 16:7801–7804.
50. Kallenius G, MoIlby R, Svenson SB, Winberg J, Hultberg H. Identification of a carbohydrate receptor recognized by uropathogenic Escherichia coli. Infection. 1980; 3:288–293. [PubMed: 6997213]
51. Old DC. Inhibition of the interaction between fimbrial hemagglutinins and erythrocytes by D-mannose and other carbohydrates. J. Gen. Microbiol. 1972; 71:149–157. [PubMed: 4556971]
52. Korhonen TK, Vaisanen-Rhen V, Rhen M, Pere A, Parkkinen J, Finne J. Escherichia coli fimbriae recognizing sialyl galactosides. J. Bacteriol. 1984; 159:762–766. [PubMed: 6146600]
53. Rhen M, Klemm P, Korhonen TK. Identification of two new hemagglutinins of Escherichia coli, N-acetyl-D-glucosamine-specific fimbriae and a blood group M-specific agglutinin, by cloning the corresponding genes in Escherichia coli K-12. J. Bacteriol. 1986; 168:1234–1242. [PubMed: 2877972]
54. Mann DA, Kanai M, Maly DJ, Kiessling LL. Probing Low Affinity and Multivalent Interactions with Surface Plasmon Resonance: Ligands for Concanavalin A. J. Am. Chem. Soc. 1998; 120:10575–10582.
55. Moscho, Alexander; Orwar, Owe; Chiu, Daniel T.; Modi, Biren P.; Zare, Richard N. Rapid preparation of giant unilamellar vesicles. Proc. Natl. Acad. Sci. USA. 1996; 93:11443–11447. [PubMed: 8876154]
56. Pevzner, Alexander; Kolusheva, Sofiya; Orynbayeva, Zulfiya; Jelinek, Raz. Membrane processes and biophysical characterization of living cells decorated with chromatic polydiacetylene vesicles. Adv. Funct. Mater. 2008:242–247.
57. Zink D, Sadoni N, Stelzer E. Visualizing chromatin and chromosomes in living cells. Methods. 2003; 29(1):42–50. [PubMed: 12543070]
58. Matthew D, Hirschey Yong-Jin Han Galen D. Stucky Alison Butler, Imaging Escherichia coli using functionalized core/shell CdSe/CdS quantum dots. J. Biol. Inorg. Chem. 2006; 11:663–669. [PubMed: 16724226]
59. Volkov VV, Asahi T, Masuhara H, Masuhara A, Kasai H, Oikawa H, Nakanishi H. Size-Dependent Optical Properties of Polydiacetylene Nanocrystal. J. Phys. Chem. B. 2004; 108:7674–7680.
60. Ma B, Fan Y, Zhang L, Kong X, Li Y, Li J. Direct colorimetric study on the interaction of Escherichia coli with mannose in polydiacetylene Langmuir-Blodgett films. Colloids and Surfaces B: Biointerfaces. 2003; 27:209–213.
61. Dogra N, Reyes JC, Garg N, Kohli P. Real-time monitoring of ligand-receptor interactions with Fluorescence Resonance Energy Transfer. J. Vis. Exp. (Not Set). :e3805. DOI: 10.3791/3805 (2012).
62. Lakowicz, JR. Principles of Fluorescence Spectroscopy. Kluwer Academics; New York: 1999. Chapter 13.

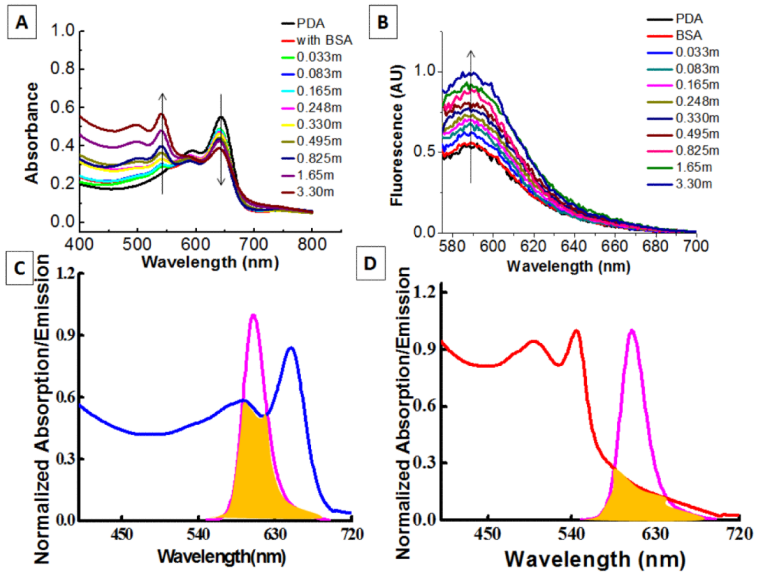

Figure 1.

Changes in the absorption (A) and emission (B) spectra of PDA liposomes (***N)*** with the addition of *E. Coli* at different concentrations. Figure 1C and 1D shows the spectral overlap (*J* value) (yellow region) between SR 101 (Pink) and Blue PDA (blue) liposome solution and spectral overlap between SR 101 and Red PDA (red) liposome solution respectively. The concentration of *E. Coli* stock solution was 3.3×10^7 *E. Coli*/mL while the concentration of BSA was 150 μg/mL. In Figure 1A and 1B, m stands for 10^7 *E.Coli* particles. For example, 0.033m means $0.033*10^7$ of *E.Coli* particles. The excitation wavelength for FRET experiments was 560 nm.

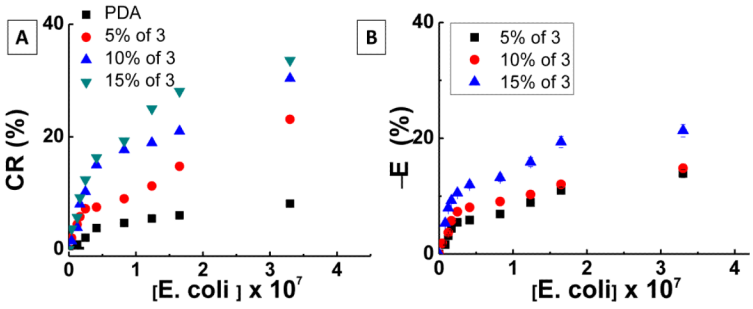

Figure 2.

(A) Colorimetric response (CR) of the liposomes-versus-*E. coli* concentration for liposomes ***N***, (B) shows FRET efficiency for liposomes *N*. Minus sign in (B) denotes a decrease in the FRET efficiency after addition of *E. Coli* to the solution. CR and ***E*** were calculated using Eqs. 1 and 3 respectively.

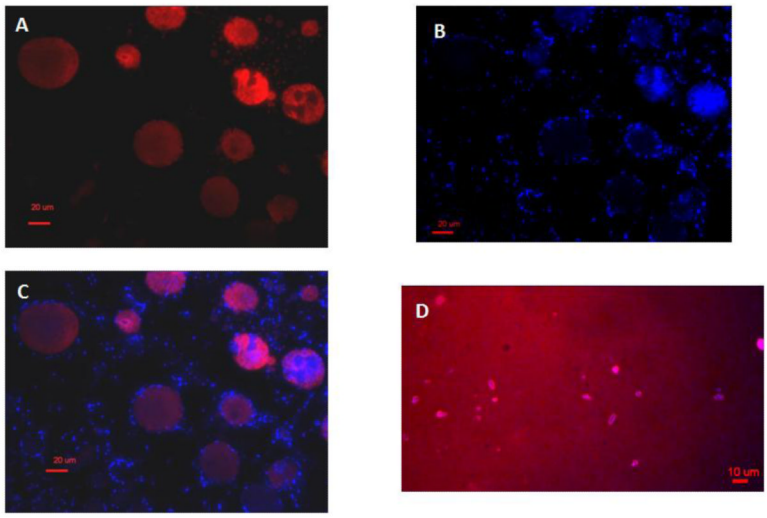

Figure 3.

(A) Fluorescence micrograph of SR-101tagged-GUV bound to excess amount of *E. Coli*. The red emission originated from SR-101. (B) DAPI-stained E. Coli bound to GUV showed blue emission. (C) Shows the composite of E. Coli-bound GUVs. (D) The fluorescence micrograph of nano-sized liposomes tagged with SR-101 bound on the surface of *E. Coli* (blue emission). Here the liposomes are totally covered with *E. Coli* surface. For these experiments, *E. Coli* was in excess (>20 times the liposome concentration). Please see experimental section for information on excitation and emission filters. The red emission was obtained using a 41004 Texas Red filter (exciting and emitting band widths of the filter used were 527-567 nm and 605-682 nm respectively). The blue emission was obtained using a DAPI filter (excitation and emission band widths were (349 ± 25) nm and (459 ± 25 nm).

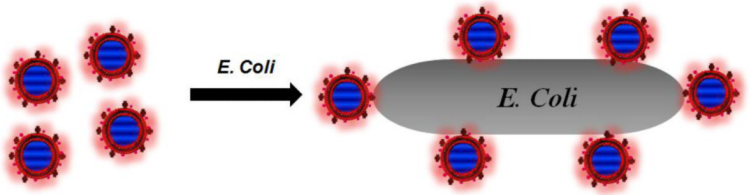

Figure 4.
The interaction of liposomes with *E. Coli* under our experimental conditions. The glucose receptors were close to the liposomal bilayer-aqueous interface such that it is proposed that, apart from specific glucose-glycoprotein interactions between liposomes and *E. Coli*, non-specific interactions are possible. The concentration of liposomes with respect to *E. Coli* concentration was low for these experiments.

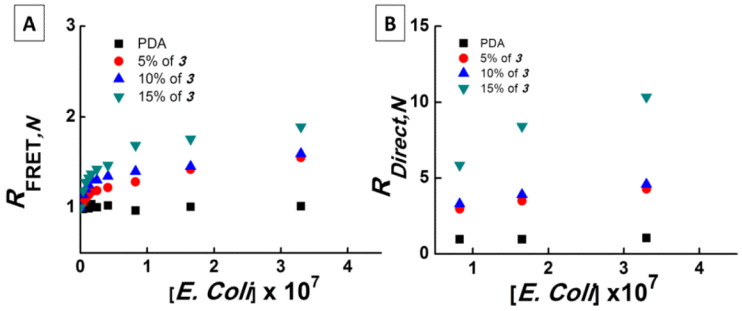

Figure 5.

(A) R_{FRET} for ***N*** series liposome at different *E. Coli* concentrations. R_{FRET} represents the ratio of SR-101 emission intensity (excitation wavelength was 560 nm) after addition of *E. Coli* of a given concentration to SR-101 emission intensity in the absence of *E. Coli*. (B) R_{Direct} at different *E. Coli* concentrations. R_{Direct} represents the ratio of PDA emission intensity (excitation wavelength was 490 nm) in the presence and absence of *E. Coli*. The excitation wavelengths for FRET and direct excitation were 560 nm and 490 nm respectively.

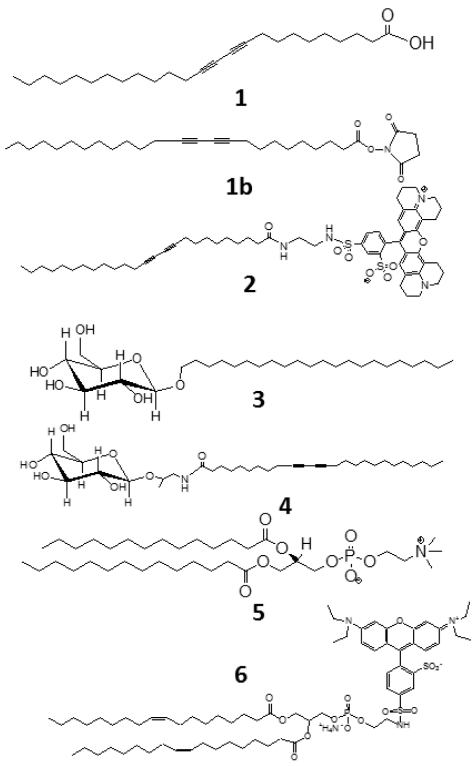

Scheme 1.
All chemicals used in the preparation of liposomes.